Available online at www.sciencedirect.com
ScienceDirect
Advances in Space Research 42 (2008) 828–832
ADVANCES IN SPACE RESEARCH (a COSPAR publication)
www.elsevier.com/locate/asr

Differential emission measure distributions in X-ray solar flares

A. Kepa *, B. Sylwester, M. Siarkowski, J. Sylwester

Space Research Centre PAS, Solar Physics Division, Wroclaw, Poland

Received 8 November 2006; received in revised form 5 April 2007; accepted 16 May 2007

Abstract

X-ray spectrometer RESIK has observed spectra in the four wavelength bands from 3.3 Å to 6.1 Å. This spectral range contains many emission lines of H- and He-like ions for Si, S, Ar and K. These lines are formed in plasma of coronal temperatures ($T > 3$ MK). Analysis of their intensities allows studying differential emission measure distributions (DEM) in temperature range roughly between 3 MK and 30 MK. The aim of present study was to check whether any relationship exists between the character of DEM distribution, the event phase and the X-ray flare class. To do this we have calculated and analyzed the DEM distributions for a set of flares belonging to different *GOES* classes from the range B5.6–X1. The DEM distributions have been calculated using "Withbroe–Sylwester" multiplicative, maximum likelihood iterative algorithm. As the input data we have used absolute fluxes observed by RESIK in several spectral bands (lines + continuum). Respective emission functions have been calculated using the CHIANTI v. 5.2 atomic data package.

Keywords: Solar flares; X-ray spectroscopy; Differential emission measure

1. Introduction

The determination of differential emission measure distributions (DEM) is groundwork for the detailed analysis of flaring plasma. The DEM $= \varphi(T)$ characterizes the distribution of matter according to the temperature T in the volume V and is defined as:

$$\varphi(T) = n_e^2 \frac{dV}{dT} \quad (1)$$

where n_e is the plasma electron density.

The calculations of the differential emission measure are associated with solving an inverse problem in which the unknown $\varphi(T)$ is the continuous function while the amount of available equations is restricted. In solving this problem many methods have been developed. They are described in the papers by: Pottasch (1964), Batstone et al. (1970), Dere et al. (1974), Doschek et al. (1990). In this paper, we calculate DEM distributions using the Withbroe–Sylwester algorithm outlined in the next section. The details one can find in the papers by Withbroe (1975) and Sylwester et al. (1980).

We have performed our study based on the X-ray fluxes observed by RESIK instrument. RESIK was Bragg crystal spectrometer aboard *CORONAS-F* satellite, which measured X-ray spectra from 3.3 Å to 6.1 Å. The description of the instrument, its calibration and the main lines identification one can find in the paper by Sylwester et al. (2005).

In the previous papers, we have focused our attention on answering the questions whether and how the durations of event (Kepa et al., 2005) and/or different ionization equilibrium approximations used to calculate the theoretical emission functions (Kepa et al., 2006) influence the resulting DEM distributions. In the present contribution our aim is to find whether the relation exists between the shape of DEM distributions, *GOES* class of event and/or the flare phase.

The theoretical emission functions applied in this study we have calculated using the CHIANTI v. 5.2 atomic data package. According to the results of previous paper (Kepa et al., 2006) the calculations of ionization equilibrium have been taken from Mazzotta et al. (1998).

* Corresponding author.
E-mail address: ak@cbk.pan.wroc.pl (A. Kepa).

0273-1177/$34.00
doi:10.1016/j.asr.2007.05.054

2. The Withbroe–Sylwester algorithm

The Withbroe–Sylwester code represents an iterative maximum likelihood procedure in which the next approximation of the DEM distribution, $\varphi_{j+1}(T)$, is calculated from preceding one, $\varphi_j(T)$, using the following formula:

$$\varphi_{j+1}(T) = \varphi_j(T)\frac{\sum_{i=1}^{k} c_i w_i(T)}{\sum_{i=1}^{k} w_i(T)} \quad (2)$$

where c_i are the correction factors taken as $c_i = F_{oi}/F_{ci}$ and $w_i(T)$ are the weight functions defined as:

$$w_i(T) = f_i(T)\varphi_j(T)\frac{\int_0^\infty f_i(T)\varphi_j(T)\mathrm{d}T}{\int_0^\infty [f_i(T)\varphi(T)]^2\mathrm{d}T} \times \left[\frac{|F_{oi} - F_{ci}|}{\sigma_i} + 1\right]^a \quad (3)$$

Here, σ_i is the uncertainty corresponding to the measured flux in line/band i ($i = 0,1,2\ldots k$) and a is the parameter of optimization: $a \geqslant 0$ for $F_{oi} \geqslant F_{ic}$ and $a < 0$ for $F_{oi} < F_{ic}$ (see Sylwester et al., 1980).

The F_{oi} is the flux observed in line/band i while the predicted flux F_{ci} is calculated (in jth iteration) using the formula:

$$F_{ci} = \int_0^\infty f_i(T)\varphi_j(T)\mathrm{d}T \quad (4)$$

where $f_i(T)$ is the emission function in line/band i.

In the calculations we have used $\varphi_0(T) = \text{const}$ as the zero approximation.

We have chosen 19 bands (wavelength intervals) for the DEM calculations. Their characteristics (wavelength ranges, and the main line contributed) are presented in Table 1. The appropriate emission functions for these spectral bands contain both line and continuum contribution.

3. The analysis

From a large RESIK database we have selected to the analysis eight representative flares of *GOES* class from B5 to X1. In Table 2 we present the main characteristics of these events ordered according to their intensity. They are: the date, *GOES* class, the maximum temperature (as determined from *GOES* data using flux ratio technique and an isothermal approximation), time intervals covering the rise, maximum and decay phases.

In order to study the DEM dependence on the flare phase we have divided each event's duration into three intervals covering the rise, maximum and the decay phase. To do this we have normalized respective *GOES* lightcurves to the common intensity scale (see Fig. 1).

After the normalization it has been easy to define the corresponding time intervals related to the rise, maximum and decay phases. The maximum phase was defined as the period when the measured flux was above the 0.9 of its maximum value. The rise/decay phases correspond to the preceding and following time intervals, respectively.

Table 1
Spectral bands used in DEM calculations

No.	Wavelength range (Å)	Main line
1	3.360–3.380	Ar XVII 3p
2	3.410–3.440	Ar XVI 3p sat.
3	3.515–3.541	K XVIII (*w*)
4	3.560–3.580	K XVIII (*z*)
5	3.680–3.710	S XVI 5p
6	3.720–3.745	Ar XVIII 2p
7	3.775–3.791	S XVI 4p
8	3.940–3.960	Ar XVI 2p
9	4.075–4.092	S XV 4p
10	4.275–4.315	S XV 3p
11	4.715–4.740	S XVI 2p
12	4.815–4.850	Si XIV 5p
13	5.010–5.075	S XV 2p (*w*)
14	5.075–5.120	S XV 2p (*z*)
15	5.200–5.240	Si XIV 3p
16	5.260–5.300	Si XIII 5p
17	5.380–5.320	Si XIII 4p
18	5.650–5.710	Si XIII 3p
19	5.790–5.845	Si XII 3p sat.

Ar XVII 3p means the $1s^2 - 1s3p$ transition in Ar XVII ion.

Table 2
The main characteristics of flares selected for the study

No.	Date	GOES class	*T* (MK)	Rise (UT)	Max (UT)	Decay (UT)
1	25 Jan. 2003	B5.6	7.6	03:06–03:08	03:08–03:10	03:10–03:15
2	11 Mar. 2003	B7.3	6.8	05:42–05:47	05:47–05:53	05:53–06:09
3	14 Feb. 2003	C1.7	11.5	06:30–06:34	06:34–06:38	06:38–06:50
4	21 Feb.2003	C4.3	14.5	19:47–19:49	19:49–19:51	19:51–19:57
5	22 Feb. 2003	C5.8	16.0	09:26–09:28	09:28–09:30	09:30–09:35
6	21 Jan. 2003	M1.9	14.0	15:10–15:21	15:21–15:33	15:33–16:04
7	07 Jan. 2003	M4.9	18.5	23:29–23:32	23:32–23:35	23:35–23:43
8	03 Aug. 2002	X1.0	19.0	19:02–19:06	19:06–19:09	19:09–19:19

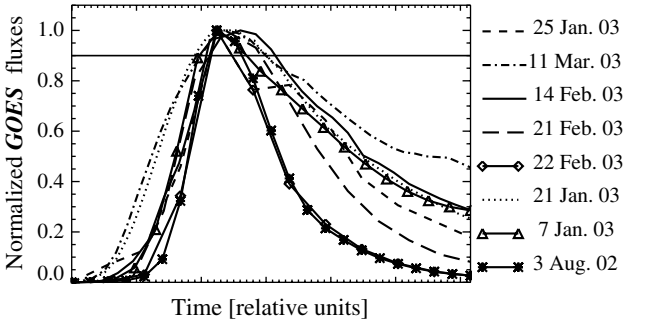

Fig. 1. The normalized standard *GOES* lightcurves for eight selected flares. The horizontal solid line at 0.9 of maximum intensity defines the flare phases (see the text for details).

In the last three columns of Table 2 corresponding intervals are indicated for analyzed flares. For DEM calculations, the spectra have been summed according to these intervals. In Fig. 2 the spectra of all flares registered during the maximum phases are presented for purpose of visual cross-comparison.

For each analyzed flare we have calculated the fluxes in selected "input" set of bands (see Table 1). This has been done separately for each of the three phases of interest (see Table 2). Additionally to avoid the contribution of non-flaring plasma to calculated DEM distributions, the preflare X-ray fluxes have been subtracted. Thus determined X-ray fluxes constitute the base for the differential emission measure calculations separately for the rise, maximum and decay phases of each event. For some flares the full data coverage have not been available because of the gaps in the RESIK data (spacecraft nights and radiation belts passages). The calculations have been performed in the range of temperatures between 2 MK and 30 MK and have been stopped after 3000 steps of iteration (χ^2 between 1 and 1.8 has been approached). The calculated DEM distributions have been plotted, carefully analyzed and compared.

In order to estimate the uncertainty of the results for each case we have performed 200 Monte-Carlo realizations of DEM calculations. The envelope of a system of obtained curves gives us the upper and lower boundary of errors. This was shown as thin lines in Fig. 3 where the calculated DEM together with the error limits are shown for the rise, maximum and decay phase of third flare from Table 2. It is seen that the flaring plasma is concentrated around two temperatures, with the low temperature component ($T<$ 5 MK) and the higher temperature component between 5 MK and 15 MK. The estimated uncertainties indicate that obtained two-component distributions can be regarded as reliable.

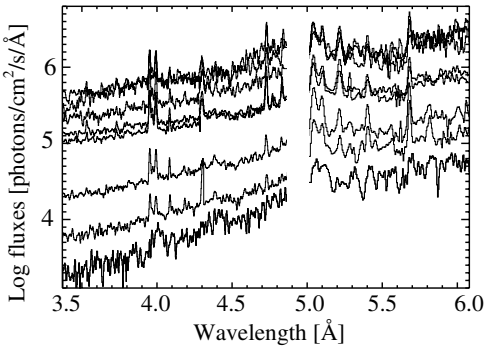

Fig. 2. The spectra of selected flares (at the maximum phase) as observed by RESIK. The bottom spectrum corresoponds to the faintest flare (No. 1 in Table 2).

4. Results and conclusions

In Fig. 4 the DEM distributions obtained for the rise, max and decay phase are presented (dotted, solid and dashed line, respectively) for eight investigated flares. In order not to obscure the results the error bars have not been presented in this figure. The inspection of Fig. 4 and corresponding analysis of the results allow for the following conclusions to be drawn:

- The calculated DEM distributions are generally two-component independent on the flare class and the evolutionary phase. This indicates for the preferential "self-concentration" of plasma into a cooler and hotter temperature regimes. The physics behind this effect is not yet clear, but most probably is related to presence of two preferred characteristic length scales important for conductive coupling of these coronal regions with the denser chromospheric-type plasma.
- The hotter component is observed to be present even for the lowest intensity B class flares, so probably such a plasma is also present in "non-flaring" active regions as well. Verification of this supposition will be a subject of a separate study. The presence of high temperature emission has been observed for active regions by *Yohkoh* (Watanabe et al., 1995).
- The "average" temperatures of cooler and hotter components are related to the flare class and clearly depend on the phase of the event. During the rise phase, the plasma is generally hotter.
- The amount of hotter plasma (i.e. integrated emission measure of a hotter component) is much smaller in comparison with the cooler one. Their relative amounts vary, depending on the flare phase and on the event class. The amount of hotter plasma is greater for the stronger flares (M, X class) in comparison with the faint ones (B, C class).
- The average temperature of the flare, as obtained based on the flux ratio technique (a standard *GOES* analysis method) is generally the indicator of physical

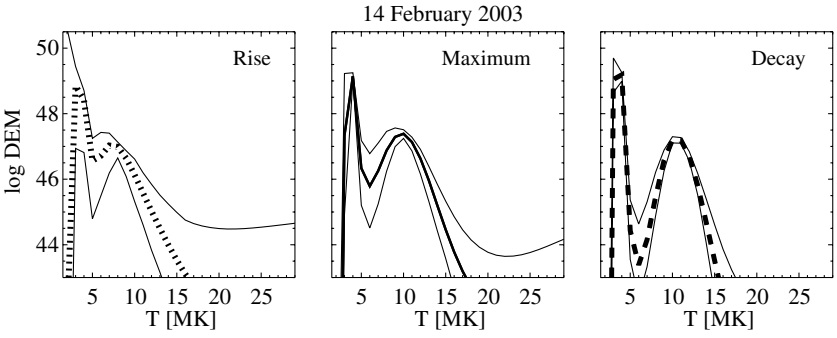

Fig. 3. The DEM distributions as calculated for rise, maximum and decay phase of 14 February 2003 flare. Thin lines correspond to the uncertainties ranges. They have been obtained from 200 Monte-Carlo realizations of DEM calculations.

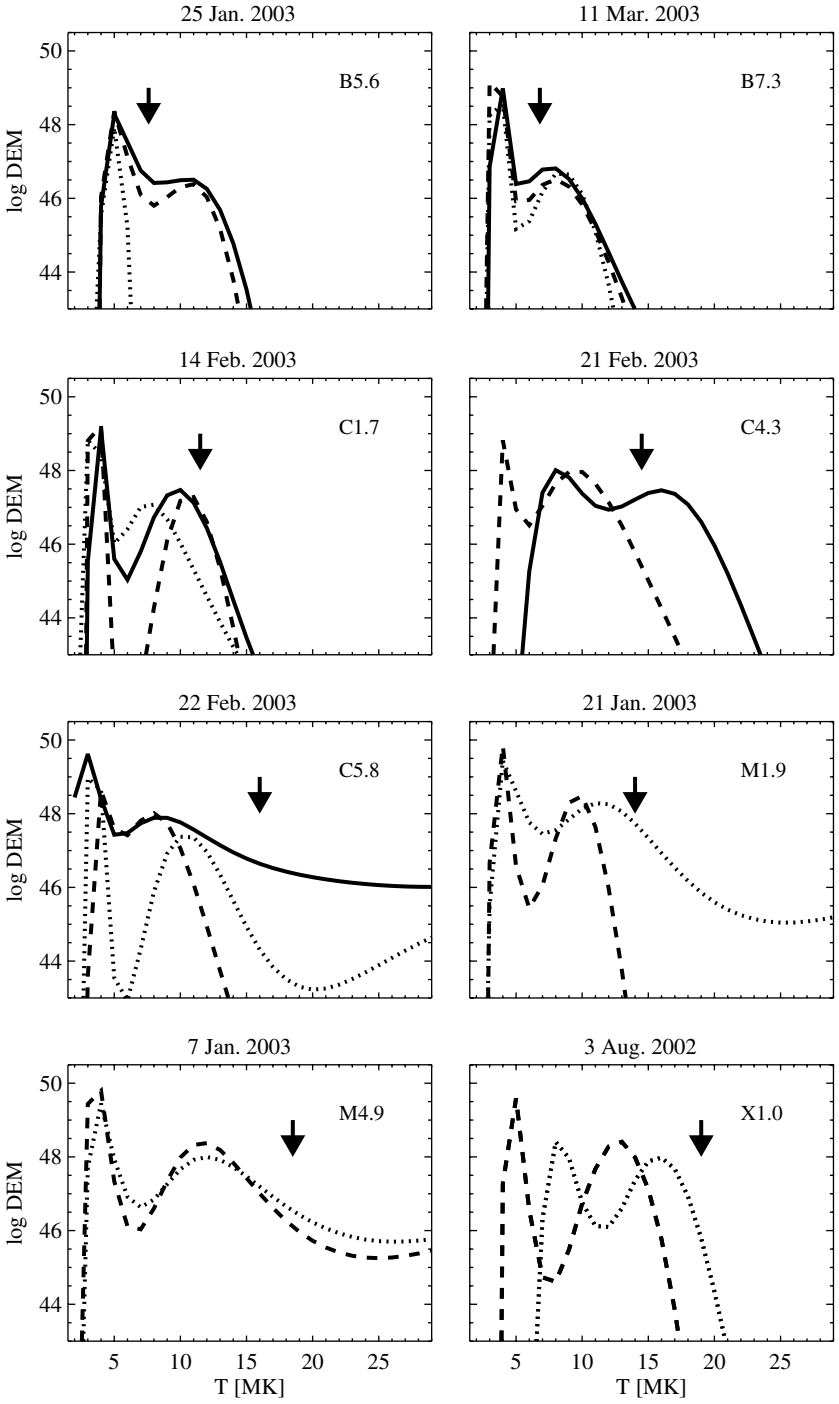

Fig. 4. The DEM distributions as calculated for eight solar flares: dotted, solid and dashed lines represent rise, maximum and decay phases respectively. Because of the satellite nights and/or radiation belts passage there are the gaps in RESIK observations so for some flares or some phases the X-ray fluxes have been not available for DEM calculations. The arrows point towards the temperatures as determined based on *GOES* fluxes ratio (see Table 2).

characteristics of the hotter component. Therefore total emission measures derived based on *GOES* fluxes are lower than those integrated from the RESIK – determined DEM distributions.

Our results are in agreement with previous works presented DEM distributions obtained based on X-rays. Schmelz (1993) calculated differential emission measure distribution for two solar flares registered by Flat Crystal Spectrometer aboard *Solar Maximum Mission*. She obtained two components distributions with lower temperature component between 3 MK and 10 MK and hotter component with temperature above 10 MK. McTiernan et al. (1999) calculated DEM distributions for 80 flares based on data from Bragg Crystal Spectrometer (BCS) and Soft X-ray Telescope aboard *Yohkoh*. For 10% of

analyzed events two-component DEM distributions have been found. The results of multithermal analysis performed for stellar corone of late type stars such as Capella, σ^2 CrB and Procyon confirmed also the dominance of plasma in two narrow temperature intervals (Mewe et al., 1986; Gu et al., 2006).

Acknowledgments

RESIK was a common project between NRL (USA), MSSL and RAL (UK), IZMIRAN (Russia) and SRC (Poland). Present study was supported by the Polish Ministry of Education and Science Grant 1.P03 D.017.29. We acknowledge unknown Referees for their remarks and comments, which allowed to clarify the reliability of presented results.

References

Batstone, R.M., Evans, K., Parkinson, J.H., Pounds, K.A. Further X-ray spectra of solar active regions. Solar Physics 13, 389–400, 1970.

Dere, P.K., Horan, D.M., Kreplin, R.W. A multi-thermal analysis of solar X-ray emission. Solar Physics 36, 459–472, 1974.

Doschek, G.A., Fludra, A., Bentley, R.D., Lang, J., Phillips, K.J.H., Watanabe, T. On the dependence of solar flare X-ray spectral line intensity ratios of highly ionized sulfur, calcium, and iron on electron temperature, differential emission measure, and atomic physics. Astrophysical Journal 358, 665–673, 1990.

Gu, M.F., Gupta, R., Peterson, J.R., Sako, M., Kahn, S.M. Capella corona revisited: A combined view from XMM-Newton RGS and Chandra HETGS and LETGS. The Astrophysical Journal 649, 979–991, 2006.

Kepa, A., Sylwester, J., Sylwester, B., Siarkowski, M., Kuznetsov, V. DEM Distributions for short and long duration flares as determined from RESIK soft X-ray spectra, in: Proceedings of the 11th European Solar Physics Meeting "The Dynamic Sun: Challenges for Theory and Observations" (ESA SP-600) Published on CDROM, 87.1, 2005.

Kepa, A., Sylwester, J., Sylwester, B., Siarkowski, M., Stepanov, A.I. Determination of differential emission measure from X-ray solar spectra registered by RESIK aboard CORONAS-F. Solar System Research 40, 294–301, 2006.

Mazzotta, P., Mazzitelli, G., Colafrancesco, S., Vittorio, N. Ionization balance for optically thin plasmas: Rate coefficients for all atoms and ions of the elements H to NI. Astronomy and Astrophysics Supplement 133, 403–409, 1998.

Mewe, R., Schrijver, C.J., Lemen, J.R., Bentley, R.D. Differential emission measure distributions of Capella and σ^2 CrB. Advances in Space Research 6, 133–136, 1986.

McTiernan, J.M., Fisher, G.H., Li, P. The solar flare soft X-ray differential emission measure and the Neupert effect at different temperatures. The Astrophysical Journal 514, 472–483, 1999.

Pottasch, S.R. On the interpretation of the solar ultraviolet emission line spectrum. Space Science Reviews 3, 816–855, 1964.

Schmelz, J.T. Elemental abundances of flaring solar plasma – Enhanced neon and sulfur. Astrophysical Journal 408, 373–381, 1993.

Sylwester, J., Gaicki, I., Kordylewski, Z., et al. RESIK: A bent crystal X-ray spectrometer for studies of solar coronal plasma composition. Solar Physics 226, 45–72, 2005.

Sylwester, J., Schrijver, J., Mewe, R. Multitemperature analysis of solar X-ray line emission. Solar Physics 67, 285–309, 1980.

Watanabe, T., Hara, H., Shimizu, T., et al. Temperature structure of active regions deduced from helium-like sulphur lines. Solar Physics 157, 169–184, 1995.

Withbroe, G.L. The analysis of XUV emission lines. Solar Physics 45, 301–317, 1975.